

## Finite-Size Scaling of the Superfluid Density of $^4\text{He}$ Confined between Silicon Wafers

Ilsu Rhee and Francis M. Gasparini

*Department of Physics and Astronomy, State University of New York at Buffalo, Buffalo, New York 14260*

David J. Bishop

*AT&T Bell Laboratories, Murray Hill, New Jersey 07974*

(Received 24 April 1989)

We report measurements of the superfluid density of  $^4\text{He}$  confined between two Si wafers. These are the first measurements of helium confined in a sufficiently well-defined planar geometry to show a crossover from three-dimensional-like to finite-size to two-dimensional behavior. Data for confinement in 0.106-, 0.509-, 2.8-, and 3.9- $\mu\text{m}$ -thickness cells are analyzed for scaling with the exponent of the bulk correlation length,  $\nu$ . We find that this scaling does not work: An exponent different from  $\nu$  is required. We discuss these results in light of finite-size scaling predictions and earlier measurements.

PACS numbers: 67.40.Hf, 05.70.Jk, 65.40.Hq

Understanding the behavior of finite systems is important in many areas of physics, both in theory and experiments. In theory, one often does numerical calculations involving a finite system and extrapolates to the thermodynamic limit. In experiments, one is often faced with a situation where one is dealing with a sample which is homogeneous only over dimensions which are comparable in size with an important length scale. For critical behavior, near a second-order transition, the growth of the correlation length produces a "rounding" of the critical-point behavior if the sample dimensions are too small. If the sample is sufficiently well defined, one can observe dimensionality crossover from three dimensions (3D) to 2D, 1D, or 0D. Bridging these limiting behaviors is a crossover region which is expected to be described by finite-size scaling theory.<sup>1</sup>

In the case of liquid helium in particular, the 2D behavior of the superfluid density of thin films has been studied as a realization of Kosterlitz-Thouless behavior.<sup>2-5</sup> There are no data on the superfluid density prior to the present work which determine the scaling with size for helium in a planar geometry. Earlier work has been on helium confined to channels where the crossover is to 1D. Previous work with helium films has yielded only the *shift* in transition temperature with film thickness, but not the finite-size aspects of a particular thermodynamic response.<sup>6</sup> An exception to this are the data on specific heat of films. These, however, are only for thicknesses up to 53 Å.<sup>7</sup> Another distinguishing feature of the present work is the fact that the helium is completely confined by rigid surfaces as opposed to the usual situation with films.

The physics we want to address with our experiment is in regard to the finite-size behavior of the superfluid density near the transition. Finite-size scaling of a system near a critical point has recently been reviewed by Barber.<sup>8</sup> For helium in particular, one may say very simply that if  $d$  is the smallest dimension of uniform

confinement, then the thermodynamic response should depend on the combination of variables  $d^\theta t$ , where  $t = |1 - T/T_\lambda|$ . One expects  $\theta^{-1} = \nu$ , if the scaling length is the 3D correlation length,  $\xi = \xi_0 t^{-\nu}$ . This kind of scaling, in fact, seems to fail for a number of experiments in helium. This is most striking for the specific heat and superfluid density of helium confined to cylindrical pores (3D to 1D crossover).<sup>7,9</sup> Most recently, Huhn and Dohm<sup>10</sup> have reported renormalization-group calculations of the specific heat for 1D crossover. They have obtained the specific heat for  $T > T_\lambda$  and the shift in the specific-heat maximum which agree with experiments. There are no calculations at present for the superfluid fraction for the case of 3D to 2D crossover.<sup>11</sup>

In the spirit of finite-size scaling we may write the superfluid fraction of the confined system,  $\rho_s/\rho$ , as

$$\frac{\rho_s}{\rho} = \frac{\rho_{sb}}{\rho} [1 - f(d^\theta t)], \quad (1)$$

where  $\rho_{sb}/\rho$  refers to the unconfined, bulk system. One must have  $f(\infty) = 0$ ; and, if this equation is to apply up to the point where  $\rho_s$  vanishes, then  $f(d^\theta t_c) = 1$  for crossover to 1D. For crossover to 2D, one might expect

$$\lim_{T \rightarrow T_c^-} f(d^\theta t) = 1 - \frac{T_c}{d\rho_{sb}} \frac{2m^2 k_B}{\pi \hbar^2}, \quad (2)$$

if one expects to have the universal jump in  $\rho_s$ .<sup>12</sup> The scaling in Eq. (1) implies a shift equation for the transition temperature,  $d^\theta t_c = \text{const}$ . In this Letter, we will concern ourselves mostly with Eq. (1). We will limit our discussion of the 2D regime to some qualitative remarks.

The design of the experimental cells used in our work is shown in Fig. 1. These cells consist of two Si wafers 0.025 cm thick and each polished on one side. One wafer is patterned lithographically to have a thin  $\text{SiO}_2$  border of 0.4-cm width, and a triangular array of  $\text{SiO}_2$  supports  $0.08 \times 0.08 \text{ cm}^2$  in cross section. These are

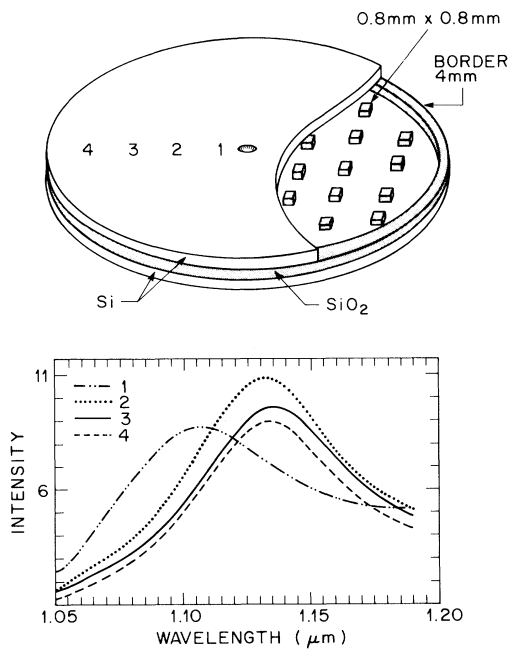


FIG. 1. Top: schematic diagram of a silicon cell. Shaded areas are  $\text{SiO}_2$ . The thickness of the oxide is not drawn to scale. Bottom: Fabry-Perot interferometer data for 3.9- $\mu\text{m}$  cell taken at four indicated positions of the cell. From the maximum we obtain the cell spacing.

spaced at 0.2-cm intervals. Another wafer with a hole through it (0.02 cm) is bonded to the patterned wafer. This process involves a chemical bond between the Si and  $\text{SiO}_2$  which forces the wafers to contour to each other.<sup>13,14</sup> This creates a pancake planar region where the helium is confined. The oxide thickness of the spacers and the border determine the cell's smallest dimension. In the case of cells with spacing  $\geq 0.6 \mu\text{m}$ , we can determine the spacing *after the bonding process* because the wafers act as a Fabry-Perot interferometer for wavelengths  $\geq 1 \mu\text{m}$  where the Si is transparent. A sample of this diagnostic is shown in Fig. 1. Here an interference fringe is obtained with a wavelength scan at four different radial positions. The maxima yield the cell's spacing. For this particular cell, the average spacing over about twenty positions along different radii is  $\bar{d} = 3.93 \pm 0.02 \mu\text{m}$ . The worst deviation,  $\pm 0.08 \mu\text{m}$ , is within 0.5 cm of the center hole where the contribution to the mechanical response of the oscillator is the least. The average spacing of the bonded cell should be compared to the oxide thickness measured with an ellipsometer after oxidation,  $\bar{d} = 3.85 \pm 0.04 \mu\text{m}$ . We consider this as excellent agreement.

To measure the superfluid mass of helium, the cell is attached to a beryllium-copper torsional element, thus forming a high- $Q$  oscillator.<sup>4</sup> This, in turn, is attached to a thermostated copper platform. Helium can be condensed into the cell through a hole in the torsion ele-

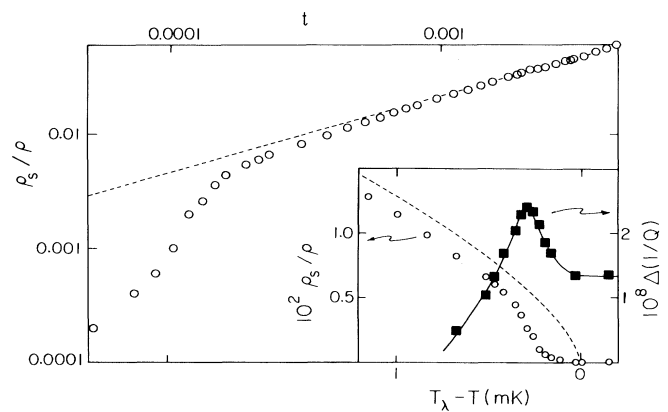


FIG. 2. Superfluid fraction vs reduced temperature for the 0.519- $\mu\text{m}$  cell. Inset: superfluid fraction and dissipation vs temperature in 2D region. The dashed lines are the expected behavior of unconfined helium. The solid line is drawn to guide the eye.

ment. To obtain the superfluid mass, one phase locks the oscillator at its resonance frequency. From the fractional period change, one can deduce the mass loading due to the helium.<sup>4</sup> This mass loading changes as the helium becomes superfluid since, in this case, only the normal-fluid portion is locked to the oscillator's movement. We report in this Letter results from four different cells of spacing 0.106, 0.519, 2.8, 3.9  $\mu\text{m}$ . These were all made of 2-in. wafers, except for the 3.9- $\mu\text{m}$  cell, which was 3 in. The fractional change in period due to the helium ranged from  $(0.26 \text{ to } 9) \times 10^{-5}$ . Our resolution was typically  $10^{-8}$ – $10^{-9}$  of the period which was in the 2–7-ms range. The oscillators with the cells loaded with helium had quality factors,  $Q$ 's in the range of  $(2 \text{ to } 8) \times 10^5$ . For two of these cells, 0.519 and 3.9  $\mu\text{m}$ , we were able to see clearly the crossover into 2D. This is marked by an increase in dissipation,  $1/Q$ .<sup>4</sup> For the two other cells the oscillator  $Q$  was not high enough for us to see this.

Data of  $\rho_s/\rho$  as function of  $t$  are shown in Fig. 2 for the 0.519- $\mu\text{m}$  cell. For large  $t$  these data match the behavior of bulk helium,  $\rho_{sb}/\rho = kt^{0.672}$  (the dashed line). In the  $10^{-3}$ – $10^{-4}$  range of  $t$ , the data begin to deviate slightly from this behavior. In the  $10^{-4}$  range this deviation is more marked. We identify this latter region as the crossover to 2D behavior. The 3D correlation length is about  $\frac{1}{3}$  the spacing of the cell at  $t = 10^{-4}$ . The 2D region is shown on a linear temperature scale as the inset in Fig. 2. Here we also plot the dissipation of the helium. We see that this peaks where  $\rho_s/\rho$  has a more abrupt deviation from 3D behavior. The dissipation in the 2D regime comes from the mechanism of vortex-antivortex unbinding.<sup>15</sup> It is tempting to identify the "break" in the  $\rho_s/\rho$  curve as the static Kosterlitz-Thouless jump at the 2D transition. However, this is not correct for these data. A more careful dynamic analysis which involves the temperature dependence of the non-

vortex superfluid density has to be done.<sup>16</sup> We do not pursue this here. For the present purpose, we view the observation of the qualitative aspects of the 2D behavior as evidence of the quality of our cells as far as homogeneity of confinement. The value of  $T_\lambda$  for this and other plots is determined *independently* in our experiment from the signature of the specific-heat singularity of a bulk sample ( $\sim 0.5 \text{ cm}^3$ ) which could be condensed on the regulated platform to which the Si cell is attached.

In Fig. 3, we have plotted the data for four cells. For clarity the data are offset by factors of 2 to avoid overlap in the power-law region. These data have similar qualitative features: a power law of  $t^{0.672}$  for large  $t$  and deviation from this at smaller  $t$ .<sup>17</sup> Note that this deviation onsets earlier, the smaller the dimension of confinement. This is as expected. To test these data against Eq. (1), we cast this in the form

$$k - \frac{\rho_s}{\rho} t^{-0.672} = f(d^{1/\nu} t), \quad (3)$$

where we have assumed bulk correlation-length scaling with  $\theta=1/\nu$ . A plot of the left-hand side of Eq. (3) vs  $d^{1/\nu} t$  is shown as the top panel of Fig. 4. *If the scaling with  $1/\nu$  were correct, these data should collapse on a single curve; they do not.* This failure of size scaling with  $1/\nu$  has been reported as well for the specific heat<sup>7</sup> and superfluid density in the case of cylindrical confinement.<sup>9</sup> We see now that this holds as well for planar confinement.

In the lower panel of Fig. 4, we plot the data with the left-hand side of Eq. (3) multiplied by  $d$ . We see now that the data do collapse reasonably well on a universal curve. Another way of seeing the lack of scaling with  $1/\nu$  is to note that if  $f(d^{1/\nu} t) \sim t^{-\nu/d}$  to leading order,<sup>9,18</sup> then the data plotted in the bottom panel of Fig. 4 should collapse on a line of slope  $-\nu$ . This is the solid line in this figure. It is clear that the data do not determine a line of this slope. If one were to force a straight

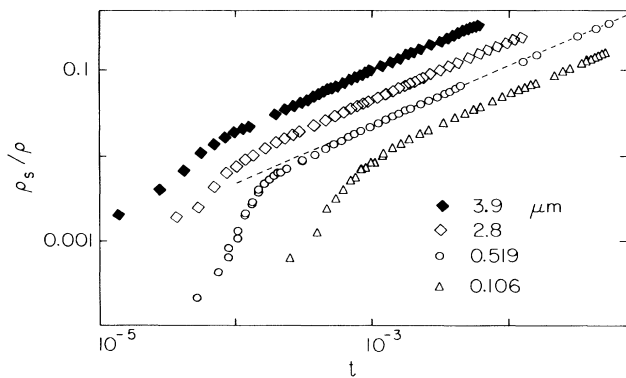


FIG. 3. Superfluid fraction vs reduced temperature for four cells. For clarity,  $\rho_s/\rho$  for the 3.9-, 2.8-, and 0.106- $\mu\text{m}$  cells are offset by a factor of 4, 2, and 0.5, respectively, relative to the data for the 0.519- $\mu\text{m}$  cell.

line through these data, one would obtain a slope of  $-1.14 \pm 0.02$ . This may be viewed as an effective exponent of 1.14 and can be compared with results from other data for planar confinement.<sup>9</sup> These yield  $1.18 \pm 0.06$  and  $0.95 \pm 0.05$ .<sup>19</sup> These seem in reasonable agreement; however, we note that the nominal confinement size given for these data is not correct as judged by the present work. This is not unexpected on the basis of the experimental arrangement used in these earlier experiments.

For  $\rho_s$  data confined to cylindrical geometry,<sup>20</sup> the analysis of Gasparini, Agnolet, and Reppy<sup>9</sup> yields an exponent of  $0.82 \pm 0.02$ . The surprising difference, however, from the present work is the fact that these data scale as  $1/d^2$  rather than as  $1/d$ . It is possible that this might be connected with the difference in the lower dimension in the case of cylinders as opposed to films. If this were so, then even the form of Eq. (1) would have to be incorrect.

Recent calculations of finite-size scaling for the Bose condensate<sup>21</sup> of the ideal Bose gas show that for non-periodic boundary conditions one needs to scale the data relative to a shifted critical temperature. We have attempted such scaling with our data relative to the temperature where  $\rho_s$  vanishes or where the dissipation is maximum. Neither of these scalings collapse the data.

In summary, we have presented new data for the superfluid density of helium confined in a well-defined planar geometry. These are the first data for such

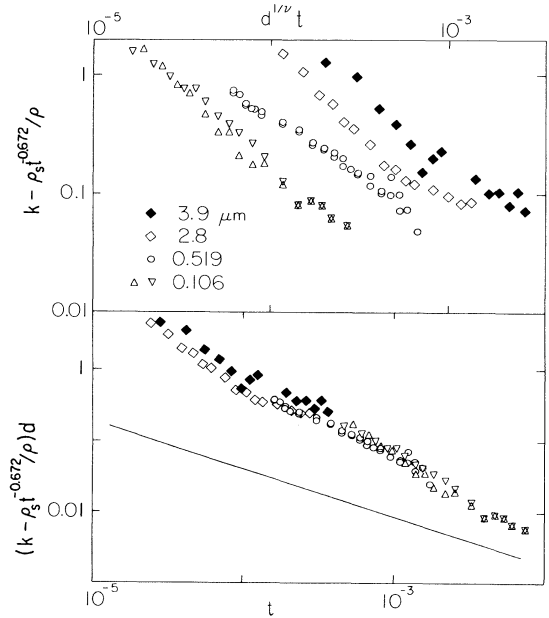


FIG. 4. Top: data plotted to test scaling with the bulk correlation length exponent  $\nu=0.672$ , Eq. (3). *The data do not collapse as expected.* Bottom: data scaled with an effective exponent of 1.14. See text.

confinement which can be scaled with size. The data display qualitative features expected for such confinement including 2D crossover. Examination of the finite-size scaling region shows that the data do not scale with  $d^{1/\nu}t$  (or equivalently  $t^{-\nu}/d$ ). We may interpret our results instead as yielding an effective exponent of  $1.14 \pm 0.02$ . When comparing with earlier work, we find this to be consistent excepting the data of Ref. 20 which scale as  $1/d^2$ . *The common features of all data for  $\rho_s$  is the lack of scaling according to Eq. (1).*

One of us, F.M.G., gratefully acknowledges the support of AT&T Bell Laboratories during a sabbatical year. We are grateful to Professor A. Petrou for his help with the infrared measurements. This work is supported in part by the National Science Foundation, Low Temperature Physics Program, Grant No. DMR8601848.

<sup>1</sup>M. E. Fisher and M. N. Barber, Phys. Rev. Lett. **28**, 1516 (1972); M. Fisher, in *Critical Phenomena*, International School of Physics "Enrico Fermi," Course 51, edited by M. S. Green (Academic, New York, 1971).

<sup>2</sup>I. Rudnick, Phys. Rev. Lett. **40**, 1454 (1978).

<sup>3</sup>D. J. Bishop and J. D. Reppy, Phys. Rev. Lett. **40**, 1727 (1978).

<sup>4</sup>D. J. Bishop and J. C. Reppy, Phys. Rev. B **22**, 5171 (1980).

<sup>5</sup>J. M. Kosterlitz and D. J. Thouless, J. Phys. C **6**, 1181 (1973).

<sup>6</sup>For a most recent discussion of the shift equation, see Y. Y. Yu, D. Finotello, and F. M. Gasparini, Phys. Rev. B **39**, 6519 (1989).

<sup>7</sup>T. P. Chen and F. M. Gasparini, Phys. Rev. Lett. **40**, 331 (1978); F. M. Gasparini, T. P. Chen, and B. Bhattacharyya, Phys. Rev. B **23**, 5797 (1981).

<sup>8</sup>M. N. Barber, in *Phase Transition and Critical Phenomena*, edited by C. Domb and J. L. Lebowitz (Academic, New York, 1983), Vol. 8.

<sup>9</sup>F. M. Gasparini, G. Agnolet, and J. D. Reppy, Phys. Rev. B **29**, 138 (1984).

<sup>10</sup>W. Huhn and V. Dohm, Phys. Rev. Lett. **61**, 1368 (1988).

<sup>11</sup>See, however, G. Williams, Phys. Rev. Lett. **59**, 1926 (1987), for a calculation of  $\rho_s$  within the Kosterlitz-Thouless theory. Finite-size effects are considered here for what we believe is 3D to 0D crossover.

<sup>12</sup>D. R. Nelson and J. M. Kosterlitz, Phys. Rev. Lett. **39**, 1201 (1977).

<sup>13</sup>R. K. Iler, *The Chemistry of Silica* (Wiley, New York, 1979).

<sup>14</sup>S. R. Hofstein, Appl. Phys. Lett. **11**, 95 (1967); R. C. Frye, J. E. Griffith, and Y. H. Wong, J. Electrochem. Soc. **133**, 1673 (1986).

<sup>15</sup>V. Ambegaokar, B. I. Halperin, D. R. Nelson, and E. D. Siggia, Phys. Rev. B **21**, 1806 (1980).

<sup>16</sup>G. Agnolet, D. F. McQueeney, and J. D. Reppy, Phys. Rev. B **39**, 8934 (1989).

<sup>17</sup>We have, in fact, used a more complete form for  $\rho_s/\rho$ , Eq. (2.3) in A. Singaas and G. Ahlers, Phys. Rev. B **30**, 5103 (1984).

<sup>18</sup>V. L. Ginzburg and A. A. Sobyenin, Usp. Fiz. Nauk. **120**, 153 (1976) [Sov. Phys. Usp. **19**, 773 (1976)].

<sup>19</sup>Data of E. N. Smith, Ph.D. thesis, Cornell University, 1971 (unpublished). Analyzed in Ref. 9.

<sup>20</sup>J. S. Brooks, B. B. Sabo, P. C. Schubert, and W. Zimmermann, Jr., Phys. Rev. B **19**, 4524 (1979).

<sup>21</sup>S. Singh and R. K. Pathria, Can. J. Phys. **63**, 358 (1985).